

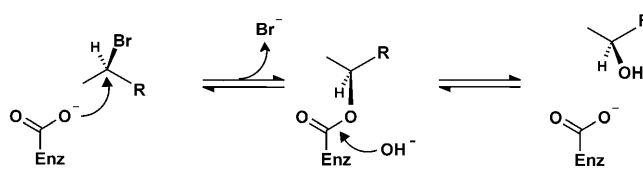
Enantioselectivity of Haloalkane Dehalogenases and its Modulation by Surface Loop Engineering**

Zbynek Prokop, Yukari Sato, Jan Brezovsky, Tomas Mozga, Radka Chaloupkova, Tana Koudelakova, Petr Jerabek, Veronika Stepankova, Ryo Natsume, Jan G. E. van Leeuwen, Dick B. Janssen, Jan Florian, Yuji Nagata, Toshiya Senda, and Jiri Damborsky*

Dedicated to Dr. Alfred Bader on the occasion of his 85th birthday

Enzymes are widely used for the synthesis of pharmaceuticals, agrochemicals, and food additives because they can catalyze enantioselective transformations.^[1] Understanding the molecular basis of enzyme–substrate interactions that contribute to enantioselectivity is important for constructing selective enzymes by protein engineering.^[2] Up to now, emphasis has been on reactions such as lipase- or esterase-based kinetic resolutions,^[2d,3] as well as lyase-, aminotransferase- and ketoreductase-mediated conversions.^[1a,4] An emerging

group of enzymes that is explored for enantioselectivity is dehalogenases. Haloalkane dehalogenases can convert a broad range of halogenated aliphatic substrates to their corresponding alcohols by an S_N2 mechanism (Scheme 1),^[5] and because of the simplicity of the reaction represent a good model system to study the structural basis of reactivity^[6] and enantioselectivity.



R = alkoxyacetyl or alkyl

Scheme 1. Reaction mechanism of haloalkane dehalogenases with α -bromoesters and β -bromoalkanes. Enz-COO⁻: active site Asp.

However, only a weak enantioselectivity (enantiomeric ratio, *E* value < 9)^[7] has been reported with haloesters and 1,2- and 1,3-dihaloalkanes for the haloalkane dehalogenases from *Xanthobacter autotrophicus* (DhlA)^[8] and *Rhodococcus rhodochrous* NCIMB13064 (DhaA).^[9] To further understand the enantioselectivity of these enzymes, we explored several dehalogenases for which the X-ray structure is available. This includes DhaA, LinB from *Sphingobium japonicum* UT26,^[10] and DbjA from *Bradyrhizobium japonicum* USDA110.^[11] Kinetic resolution of an expanded set of racemic substrates was analyzed with recombinant proteins, and it revealed that DhaA, LinB, and DbjA possess excellent enantioselectivity for α -bromoesters (Table 1). Furthermore, DbjA showed high enantioselectivity with two β -bromoalkanes.

The steady-state kinetics of DbjA determined with (*R*)- and (*S*)-2-bromopentane showed a large difference in Michaelis constants *K_m* (24 and 570 μ M, respectively) and similar catalytic constants *k_{cat}* (0.36 and 0.27 s⁻¹), which indicates that enantioselectivity in this case is mainly the result of substrate binding. The high enantioselectivity of DbjA allowed use of the enzyme for kinetic resolution of 2-bromopentane on a preparative scale. Incubation of racemic substrate (7 g) in a 4:1 mixture of Tris buffer (24 L, 50 mM, pH 8.2) and dimethyl sulfoxide with DbjA enzyme (240 mg as extract of *Escherichia coli* cells) at room temperature gave complete conversion of the *R* enantiomer (> 99% *ee*) after

[*] Dr. Z. Prokop,^[†] J. Brezovsky,^[†] T. Mozga, Dr. R. Chaloupkova, T. Koudelakova, P. Jerabek, V. Stepankova, Prof. J. Damborsky Loschmidt Laboratories, Department of Experimental Biology and Centre for Toxic Compounds in the Environment Faculty of Science, Masaryk University Kamenice 5/A13, 625 00 Brno (Czech Republic) Fax. (+420) 5-4949-2556

E-mail: jiri@chemi.muni.cz

Homepage: <http://loschmidt.chemi.muni.cz/peg>

Dr. Y. Sato,^[†] Dr. Y. Nagata

Department of Life Sciences, Graduate School of Life Sciences, Tohoku University, Sendai (Japan)

Dr. Y. Sato,^[†] Dr. R. Natsume

Japan Biological Informatics Consortium, Tokyo (Japan)

J. G. E. van Leeuwen, Prof. D. B. Janssen

Department of Biochemistry, University of Groningen (The Netherlands)

Dr. J. Florian

Department of Chemistry, Loyola University Chicago (USA)

Dr. T. Senda

Biomedical Information Research Center, National Institute of Advanced Industrial Science and Technology, Tokyo (Japan)

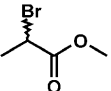
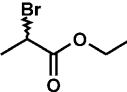
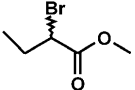
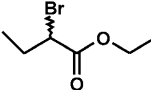
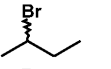
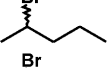
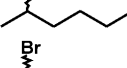
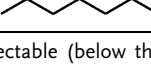
[†] These authors contributed equally to this work.

[**] Z.P. acknowledges EMBO for financial support of his stay at the University of Groningen. Financial support is gratefully acknowledged from: the Ministry of Education, Youth, and Sports of the Czech Republic (grants LC06010 to J.D. and MSM0021622412 to Z.P.); the Grant Agency of the Czech Academy of Sciences (grant no. IAA401630901 to J.B.); the Grants-in-Aid from Ministry of Education, Culture, Sports, Science, and Technology, Japan and the Ministry of Agriculture, Forestry, and Fisheries, Japan (Y.N.); and the New Energy and Industrial Technology Development Organization (NEDO) of Japan (T.S.). Access to the METACentrum supercomputing facilities is highly appreciated (MSM6383917201). We thank Prof. Uwe Bornscheuer from the University of Greifswald for critical reading of this manuscript.



Supporting information for this article is available on the WWW under <http://dx.doi.org/10.1002/anie.201001753>.

Table 1: Enantioselectivity of haloalkane dehalogenases DhaA, LinB, and DbjA towards β -bromoalkanes and α -bromoesters.^[a]

	<i>E</i> value	DhaA <i>ee</i> [%]	<i>c</i> [%]	<i>E</i> value	LinB <i>ee</i> [%]	<i>c</i> [%]	<i>E</i> value	DbjA <i>ee</i> [%]	<i>c</i> [%]	
α -bromoesters		> 200	> 99	54	52	92	51	> 200	> 99	51
		85	97	50	97	95	51	> 200	> 99	50
		n.d.	n.d.	n.d.	28	88	51	> 200	97	54
		> 200	> 99	51	> 200	> 99	51	> 200	> 99	50
β -bromoalkanes		2	24	57	2	16	56	1	7	50
		7	79	61	16	80	53	145	> 99	53
		4	43	60	12	53	55	68	90	50
		3	41	48	3	39	51	28	80	50

[a] n.d. = no activity detectable (below the detection limit of $0.5 \text{ nmol min}^{-1} \text{ mg}^{-1}$ of enzyme). The enantiomeric ratio (*E* value) is a quantitative measure of enzyme stereospecificity and its relationship with enantiomeric excess (*ee*) and degree of conversion (*c*) has been described.^[12] See the Supporting Information for a complete list of tested substrates.

150 minutes.^[13] Subsequent extraction and purification yielded the pure *S* enantiomer (21% yield, purity 86%, > 99% *ee*).

To dissect the molecular basis of DbjA enantioselectivity, we undertook a detailed analysis using kinetic measurements, mutagenesis, protein crystallography, thermodynamic analysis, and molecular modeling. We selected 2-bromopentane and methyl 2-bromobutyrate as representative substrates for β -bromoalkanes and α -bromoesters, respectively.

A sequence alignment of haloalkane dehalogenases suggested that the high enantioselectivity of DbjA arises from an additional segment between the core α/β -hydrolase and cap domains (Figure 1 a). The crystal structure of DbjA revealed that this segment is located on the protein surface and does not directly take part in shaping the active-site pocket (Figure 1 b). The effect of loops on enzyme enantioselectivity has been reported,^[2h] which let us construct a deletion mutant (DbjA Δ) lacking the fragment 140-His-Thr-Glu-Val-Ala-Glu-Glu-146 (hereafter termed the EB fragment, Extra region of *B. japonicum*, Figure 1 a) in this region. Indeed, the deletion of the fragment changed the enantioselectivity with both substrates (Figure 2 a,b). Surprisingly, an inverse effect of the deletion was observed with two representative substrates: decreased enantioselectivity with 2-bromopentane and increased enantioselectivity with methyl 2-bromobutyrate (Figure 2 a,b).

The crystal structure of DbjA Δ shows that deletion of the EB fragment alters the shape and size of the active-site pocket

(Figure 1 b). This change mainly arises from modulation of the conformational behavior of His139, located next to the deleted fragment. His139 adopts two different conformations, inclined and deflected, in DbjA, whereas only the inclined conformation can be seen in DbjA Δ (Figure 1 c). Deletion of the loop region resulted in a reduction of the volume of the space that accommodates the side chain of His139 (Figure 1 d).

Thermodynamic analysis of the reactions revealed that enantiodiscrimination of methyl 2-bromobutyrate arises from nearly identical enthalpy–entropy contributions in both the wild type and deletion mutant (Figure 2 a,b). In both cases, the difference in transition-state enthalpy ($\Delta_{R-S}\Delta H^\ddagger$) supports preferential conversion of the *R* enantiomer, while entropy promotes conversion of the *S* enantiomer.

The thermodynamic characteristics of the reaction with 2-bromopentane were significantly changed by the mutation. The preferential conversion of the *R* enantiomer found with wild-type DbjA is because of a stronger enthalpic contribution to transition-state stabilization, which is partially suppressed by entropy favoring the *S* enantiomer (Figure 2 a,b). Strikingly, in DbjA Δ , the enthalpic contribution to enantioselectivity is opposite to that for the wild type, thus resulting in a reversed temperature dependence of the *E* value that has rarely been observed (Figure 2 a,b).^[16] Enantiopreference was preserved in the deletion mutant since the entropic contribution is also opposite and becomes dominant, now strongly favoring the enantiopreference of the *R* enantiomer. The

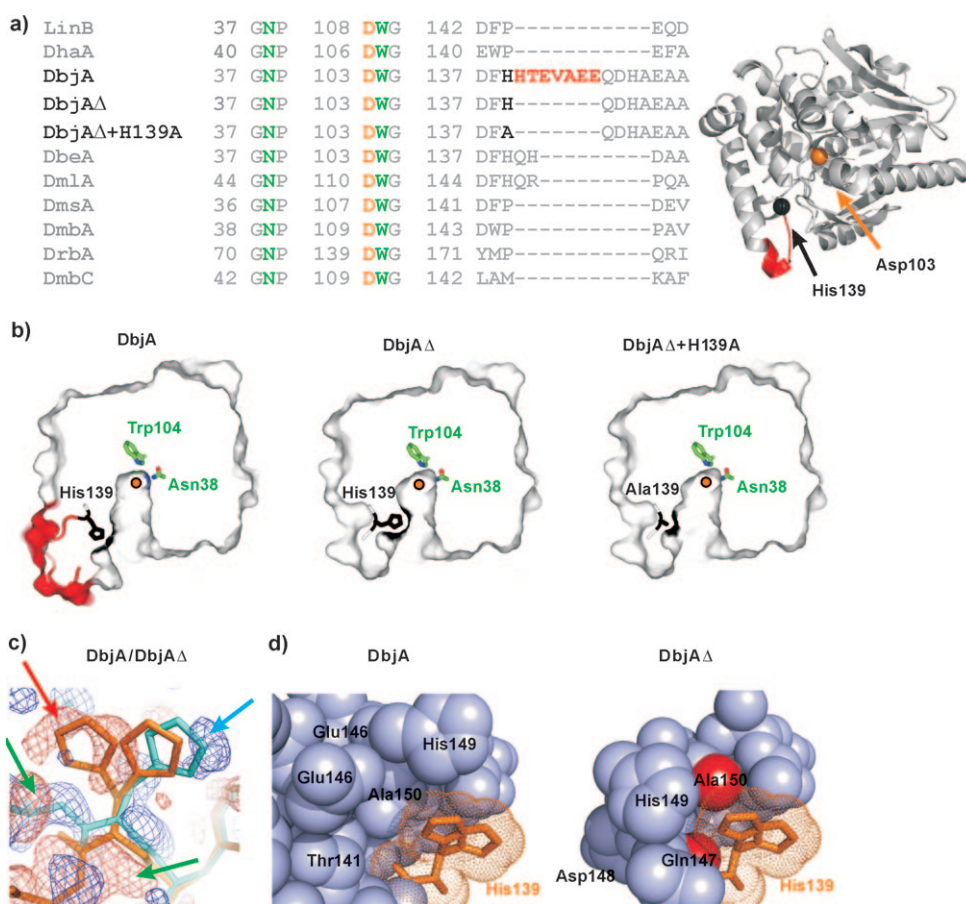


Figure 1. Structural comparison of haloalkane dehalogenases. a) The amino acid sequence alignment of haloalkane dehalogenases LinB,^[10] DhaA,^[9] DbjA,^[11] DbjA Δ , DbjA Δ +His139Ala (this study, PDB ID 3A2M and 3A2L), DbeA (Ikeda-Ohtsubo et al., unpublished), DmlA,^[11] DmsA, DmbA,^[14] DrbA, and DmbC.^[15] Halide-stabilizing Asn and Trp residues are shown in green, the nucleophile in orange, the EB fragment deleted in DbjA Δ in red, and the residue 139 in black (left panel). The right-hand panel shows the overall structure of DbjA with the deleted residues within the EB loop in red. b) Active-site structures of haloalkane dehalogenases. The nucleophile (Asp103) is depicted as an orange dot. His139 can adopt inclined and declined conformations, which affects the size and hydrophobicity of the active-site pocket. c) F_o (DbjA)– F_o (DbjA Δ) difference Fourier maps, contoured at 3.0σ (red) and -3.0σ (blue), around His139 of DbjA (orange) and DbjA Δ (cyan). Red density indicated by red arrows suggests that the deflected conformation of His139 (His139-II) in DbjA has higher occupancy than in DbjA Δ . Blue density indicated by blue arrows suggests that the inclined conformation of His139 (His139-I) in DbjA Δ has higher occupancy than in DbjA. Densities indicated by green arrows indicate the difference in the polypeptide chain conformation between DbjA and DbjA Δ . d) Deletion of the EB fragment affects the conformation of His139 (orange). The model structures of two alternative conformations of His139 in DbjA Δ were prepared on the basis of the crystal structure of DbjA. Deflected His139 in DbjA Δ makes close contacts with the N atom of Gln147 and the C β atom of Ala150 (red). See the Supporting Information for details of structural analysis.

results of thermodynamic and mutagenesis analysis indicate that the enantioselective reactions with 2-bromopentane and methyl 2-bromobutyrate are controlled by different molecular bases.

Next, we tried to link these molecular bases to three-dimensional structures of wild-type and mutant DbjA by molecular modeling. Both enantiomers of 2-bromopentane bind along the same wall of the active-site pocket, and adopt a mirror-image orientation with displaced chiral centers (Figure 2c). This binding is characterized by hydrophobic interactions between the alkyl chain of the substrate and the

hydrophobic wall, and by two hydrogen bonds between the bromine atom and the side chains of the halide-stabilizing residues Trp104 and Asn38. During the molecular dynamics simulation, the *R* enantiomer was sampled exclusively in a reactive binding mode, while (*S*)-2-bromopentane adopted a mixture of reactive and nonreactive binding modes. His139 appeared to modulate the distribution of reactive configurations^[17] among these binding modes by its interaction with the substrate molecule (Figure 2c, Supporting Information Figure 1). The simulations showed that the inclined conformation of His139 in DbjA Δ decreases reactivity with the *R* enantiomer and increases reactivity with the *S* enantiomer (Supporting Information Figure 3 and Table 3), which results in reduced enantioselectivity of this mutant with 2-bromopentane. The effect of the mutation is opposite for the two enantiomers because of the different location of their chiral centers (Figure 2c).

In contrast to what was observed with 2-bromopentane, the enantiomers of methyl 2-bromobutyrate appeared to bind in different orientations with their chiral centers aligned and the two substituting alkyl groups pointing towards different sides of the active site (Figure 2c). These orientations are stabilized by three hydrogen bonds: two between bromine and the side chains of halide-stabilizing residues, and one between the substrate carbonyl group and the side chain of Asn38 or Trp104 for the *R* and *S* enantiomer, respectively (Figure 2c, Supporting Information Figure 1). Hydrophobic interactions with the wall of the active-site pocket are less important for methyl 2-bromobutyrate than for 2-bromopentane. The binding free energies calculated for these binding modes favor binding of the *R* enantiomer over the *S* enantiomer, irrespective of the protein variant, because of better conformity of the *R* enantiomer with the active site. The discrimination against the

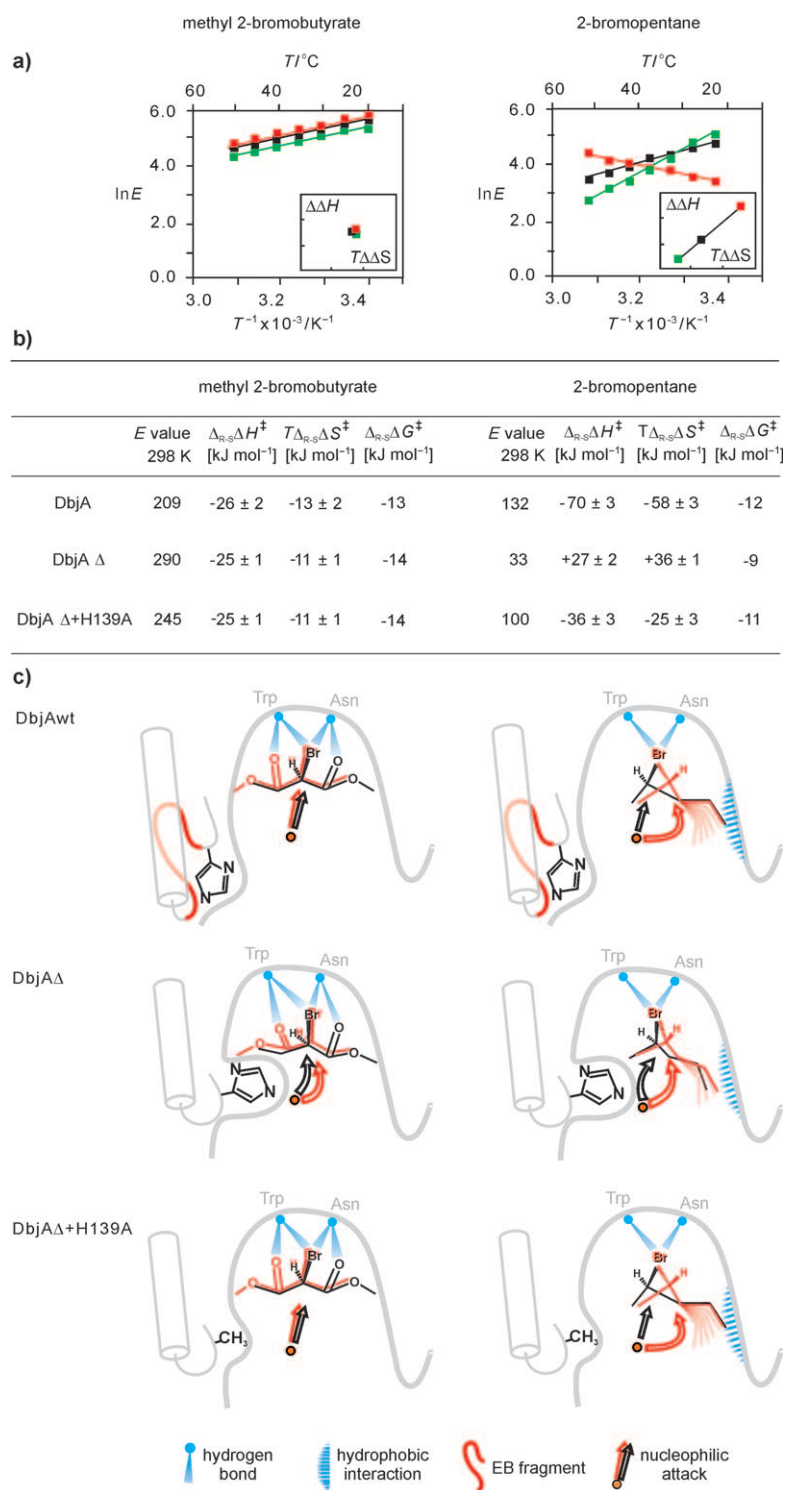


Figure 2. Two molecular bases of enantioselectivity of haloalkane dehalogenases. a) Thermodynamic analysis of the reactions catalyzed by DbjA (green), DbjAΔ (red), and DbjAΔ + His139Ala (black) with methyl 2-bromobutyrate (left) and 2-bromopentane (right) illustrates the temperature dependence of their enantiomeric ratios and the enthalpy–entropy compensation (in the insets). b) Thermodynamic components of the enantioselectivity of DbjA, DbjAΔ, and DbjAΔ + His139Ala: enantioselectivity (E value), differential transition state free energy ($\Delta_{R-S}\Delta G^\ddagger = \Delta_{R-S}\Delta H^\ddagger - T\Delta_{R-S}\Delta S^\ddagger$) and its enthalpic ($\Delta_{R-S}\Delta H^\ddagger$) and entropic ($T\Delta_{R-S}\Delta S^\ddagger$) contributions at $T = 298$ K. c) Mutations have distinct effects on the active-site pocket, binding orientations, and reactivity of R enantiomers (black) and S enantiomers (red).

S enantiomer is further reinforced in the chemical step of the reaction (Supporting Information Table 3). The inclined conformation of His139 in DbjAΔ decreases reactivity with both enantiomers since their chiral centers are spatially aligned. The magnitude of this effect is larger for the S enantiomer, thus resulting in increased enantioselectivity with methyl 2-bromobutyrate (Supporting Information Figure 2 and Table 3).

Our analysis of DbjA enantioselectivity demonstrates that different molecular bases underlie the enantioselective conversion of methyl 2-bromobutyrate and 2-bromopentane (Figure 2c). Furthermore, the enantioselectivity of DbjA can be modulated by mutation at the surface loop region. Assuming that the inclined conformation of His139 in DbjAΔ significantly reduces the volume of the active-site pocket, substitution of His139 by Ala should restore the original enzyme enantioselectivity. Indeed, the enantioselectivity of the DbjAΔ + His139Ala mutant was reconstituted for both substrates (Figure 2a,b). The effects of the mutations were stronger for 2-bromopentane than for methyl 2-bromobutyrate because of different binding orientations and the distinct nature of the interactions involved in their enantiodiscrimination.

In conclusion, we have shown that haloalkane dehalogenases: 1) can kinetically discriminate between enantiomers of two distinct groups of substrates, α -bromoesters and β -bromoalkanes; 2) have enantioselectivity based on distinct molecular interactions, which can be modified separately by engineering of a surface loop; and 3) can adopt an inverse temperature dependence of enantioselectivity for β -bromoalkanes, but not α -bromoesters, by mutating this surface loop and a flanking residue. Our study contributes towards understanding of the molecular basis and thermodynamics of the enantioselectivity of enzymes,^[18] and opens up new possibilities for constructing enantioselective biocatalysts by protein engineering.

Received: March 24, 2010

Published online: July 19, 2010

Keywords: enantioselectivity · enzymes · haloalkane dehalogenases · protein engineering · thermodynamics

[1] a) K. Faber, *Biotransformations in Organic Chemistry*, Springer, Heidelberg, **2000**; b) H. E. Schoemaker, D. Mink, M. G. Wubbolts, *Science* **2003**, 299, 1694–1697.

[2] a) R. J. Kazlauskas, *Trends Biotechnol.* **1994**, 12, 464–472; b) W. V. Tuomi, R. J. Kazlauskas, *J. Org. Chem.* **1999**, 64, 2638–2647; c) D. Rotticci, J. C. Rotticci-Mulder, S. Denman, T. Norin, K. Hult,

- ChemBioChem* **2001**, *2*, 766–770; d) U. T. Bornscheuer, *Curr. Opin. Biotechnol.* **2002**, *13*, 543–547; e) E. Henke, U. T. Bornscheuer, R. D. Schmid, J. Pleiss, *ChemBioChem* **2003**, *4*, 485–493; f) K. Hult, P. Berglund, *Curr. Opin. Biotechnol.* **2003**, *14*, 395–400; g) T. Ema, T. Fujii, M. Ozaki, T. Korenaga, T. Sakai, *Chem. Commun.* **2005**, 4650–4651; h) Y. L. Boersma, T. Pijning, M. S. Bosma, A. M. van der Sloot, L. F. Godinho, M. J. Dröge, R. T. Winter, G. van Pouderooyen, B. W. Dijkstra, W. J. Quax, *Chem. Biol.* **2008**, *15*, 782–789; i) M. T. Reetz, M. Bocola, L. W. Wang, J. Sanchis, A. Cronin, M. Arand, J. Zou, A. Archelas, A. L. Bottalla, A. Naworyta, S. L. Mowbray, *J. Am. Chem. Soc.* **2009**, *131*, 7334–7343.
- [3] M. T. Reetz, *Curr. Opin. Chem. Biol.* **2002**, *6*, 145–150.
- [4] H. Iding, P. Siegert, K. Mesch, M. Pohl, *Biochim. Biophys. Acta Protein Struct. Mol. Enzymol.* **1998**, *1385*, 307–322.
- [5] J. Damborsky, E. Rorije, A. Jesenska, Y. Nagata, G. Klopman, W. J. G. M. Peijnenburg, *Environ. Toxicol. Chem.* **2001**, *20*, 2681–2689.
- [6] a) J. Damborsky, M. Kutý, M. Nemeč, J. Koca, *J. Chem. Inf. Comput. Sci.* **1997**, *37*, 562–568; b) F. C. Lightstone, Y. Zheng, T. C. Bruice, *J. Am. Chem. Soc.* **1998**, *120*, 5611–5621; c) M. Otyepka, J. Damborský, *Protein Sci.* **2002**, *11*, 1206–1217; d) A. Shurki, M. Strajbl, J. Villà, A. Warshel, *J. Am. Chem. Soc.* **2002**, *124*, 4097–4107; e) K. Nam, X. Prat-Resina, M. Garcia-Viloca, L. S. Devi-Kesavan, J. Gao, *J. Am. Chem. Soc.* **2004**, *126*, 1369–1376; f) A. Soriano, E. Silla, I. Tuñón, M. F. Ruiz-López, *J. Am. Chem. Soc.* **2005**, *127*, 1946–1957; g) A. Negri, E. Marco, J. Damborsky, F. Gago, *J. Mol. Graphics Modell.* **2007**, *26*, 643–651; h) M. Klvana, M. Pavlova, T. Koudelakova, R. Chaloupkova, P. Dvorak, Z. Prokop, A. Stsiapanava, M. Kutý, I. Kuta-Smatanova, J. Dohnalek, P. Kulhanek, R. C. Wade, J. Damborsky, *J. Mol. Biol.* **2009**, *392*, 1339–1356.
- [7] R. J. Pieters, J. H. L. Spelberg, R. M. Kellogg, D. B. Janssen, *Tetrahedron Lett.* **2001**, *42*, 469–471.
- [8] S. Keuning, D. B. Janssen, B. Witholt, *J. Bacteriol.* **1985**, *163*, 635–639.
- [9] A. N. Kulakova, M. J. Larkin, L. A. Kulakov, *Microbiology* **1997**, *143*, 109–115.
- [10] Y. Nagata, K. Miyauchi, J. Damborsky, K. Manova, A. Ansovgova, M. Takagi, *Appl. Environ. Microbiol.* **1997**, *63*, 3707–3710.
- [11] Y. Sato, M. Monincova, R. Chaloupkova, Z. Prokop, Y. Ohtsubo, K. Minamisawa, M. Tsuda, J. Damborsky, Y. Nagata, *Appl. Environ. Microbiol.* **2005**, *71*, 4372–4379.
- [12] C. S. Chen, Y. Fujimoto, G. Girdaukas, C. J. Sih, *J. Am. Chem. Soc.* **1982**, *104*, 7294–7299.
- [13] Z. Prokop, J. Damborsky, D. B. Janssen, Y. Nagata, US7,632,666, **2009**.
- [14] A. Jesenska, M. Pavlova, M. Strouhal, R. Chaloupkova, I. Tesinska, M. Monincova, Z. Prokop, M. Bartos, I. Pavlik, I. Rychlik, P. Mobius, Y. Nagata, J. Damborsky, *Appl. Environ. Microbiol.* **2005**, *71*, 6736–6745.
- [15] A. Jesenska, J. Sykora, A. Olzynska, J. Brezovsky, Z. Zdrahal, J. Damborsky, M. Hof, *J. Am. Chem. Soc.* **2009**, *131*, 494–501.
- [16] a) V. T. Pham, R. S. Phillips, *J. Am. Chem. Soc.* **1990**, *112*, 3629–3632; b) R. S. Phillips, *J. Mol. Catal. B* **2002**, *19–20*, 103–107; c) A. O. Magnusson, M. Takwa, A. Hamberg, K. Hult, *Angew. Chem.* **2005**, *117*, 4658–4661; *Angew. Chem. Int. Ed.* **2005**, *44*, 4582–4585.
- [17] S. Hur, K. Kahn, T. C. Bruice, *Proc. Natl. Acad. Sci. USA* **2003**, *100*, 2215–2219.
- [18] a) G. Gartler, C. Kratky, K. Gruber, *J. Biotechnol.* **2007**, *129*, 87–97; b) R. M. de Jong, J. J. Tiesinga, A. Villa, L. Tang, D. B. Janssen, B. W. Dijkstra, *J. Am. Chem. Soc.* **2005**, *127*, 13338–13343; c) I. Ivanov, S. Romanov, C. Ozdoba, H. G. Holzhutter, G. Myagkova, H. Kuhn, *Biochemistry* **2004**, *43*, 15720–15728; d) S. V. Singh, V. Varma, P. Zimniak, S. K. Srivastava, S. W. Marynowski, D. Desai, S. Amin, X. Ji, *Biochemistry* **2004**, *43*, 9708–9715; e) H. J. Yang, T. Matsui, S. Ozaki, S. Kato, T. Ueno, G. N. Phillips, Jr., S. Fukuzumi, Y. Watanabe, *Biochemistry* **2003**, *42*, 10174–10181; f) I. G. Muñoz, S. L. Mowbray, J. Stahlberg, *Acta Crystallogr. Sect. D* **2003**, *59*, 637–643; g) J. Ståhlberg, H. Henriksson, C. Divne, R. Isaksson, G. Pettersson, G. Johansson, T. A. Jones, *J. Mol. Biol.* **2001**, *305*, 79–93; h) M. Sundaramoorthy, J. Turner, T. L. Poulos, *Chem. Biol.* **1998**, *5*, 461–473; i) D. A. Lang, M. L. Mannesse, G. H. de Haas, H. M. Verheij, B. W. Dijkstra, *Eur. J. Biochem.* **1998**, *254*, 333–340; j) M. Holmquist, F. Haefner, T. Norin, K. Hult, *Protein Sci.* **1996**, *5*, 83–88.